JOURNAL OF MATERIALS SCIENCE **37** (2002) 5229–5236

Microstructure and mechanical properties of chromium and chromium/nickel particulate reinforced alumina ceramics

Y. JI*, J. A. YEOMANS
School of Engineering, University of Surrey, Guildford, Surrey, GU2 7XH, UK

A range of Al_2O_3-Cr and Al_2O_3-Cr/Ni composites have been made using either pressureless sintering in the presence of a graphite bed or hot pressing. Examination of the microstructures shows that they are fully dense (typically 98–99% of the theoretical density) and that the micrometre-scale metallic particles remain discrete and homogeneously dispersed in all composites. All of the hot pressed specimens had higher flexural strengths than the sintered materials. Within each processing route, the composites had slightly lower strength values than the equivalent monolithic alumina specimens. This was attributed to weak interfacial bonding. Fracture toughness behaviour was investigated using indentation and double cantilever beam methods. All of the composites were found to be tougher than the parent alumina and to show resistance-curve behaviour. For the composites, maximum fracture toughness values were 5–6 MPa $m^{1/2}$ (about double the value for alumina) for process zone sizes of a few millimetres, although steady state was not reached in the limited number of specimens tested. Examination of fracture surfaces and indentation cracks showed that the toughening potential of the metal particles was not exploited to any significant extent. This was mainly due to weak metal-Al_2O_3 interfaces, but also because of carbon embrittlement of the metallic particles in which chromium was the major constituent.

1. Introduction

As the use of ceramics as structural materials is often limited by their brittleness, much effort has been directed towards producing tougher ceramics. The fracture toughness of the matrix materials can be improved by incorporating various energy-dissipating components into the microstructure to create ceramic matrix composites. Among these mechanisms, incorporation of a metallic phase has been shown to be one of the promising methods to toughen brittle materials. Toughening is most effective when the crack is bridged by intact ligaments of the ductile phase behind the advancing crack tip. If the metallic phase is continuous it cannot be by-passed by an advancing crack and this ensures utilisation of the crack bridging mechanism. The presence of a continuous metal phase, however, is not always desirable as it can lead to problems associated with electrical conductivity, environmental degradation and creep. Thus, it can be desirable to have the second phase in the form of discrete particles.

Alumina is the most common matrix material to be studied and within the discrete metal particle category of composites, there have been a number of reports on the effects of different metals including Ni[1–8], Ni-Co [9, 10], Fe [11–13], Fe-Cr [13], Cr [14] , Ag [15], Mo [16–18], Cu [19–21] and W [22, 23]. Whilst earlier work tended to use particles in the micrometre-scale range, over the last decade there has been increasing interest in using particles in the nanometre-scale range. Such nanocomposites tend to be stronger, as a result of the matrix grain size refinement resulting from the pinning effect of the particles, but the toughness of these materials is not improved significantly.

The present work concerns the microstructure and its effect on the mechanical properties of Al_2O_3-Cr and Al_2O_3-Cr/Ni composites with Cr particle sizes in the micrometre size range. Chromium has been selected because it has a coefficient of thermal expansion [24] that is lower than that for alumina [25] at room temperature, unlike many of the other metals that have been used in previous programmes. The coefficient of thermal expansion is higher than alumina at higher temperatures but, nevertheless, the residual stresses developed as a result of the mismatch in the coefficients of thermal expansion should be lower than for other alumina-metal systems and might even lead to cracks being attracted to the metallic particles, thus encouraging utilisation of the ductile bridging mechanism. Furthermore, Al_2O_3 and Cr_2O_3 are completely soluble in each other and this may aid the formation of a strong bond between Al_2O_3 and Cr.

Present address: Department of Materials, Imperial College of Science, Technology and Medicine, Prince Consort Road, London SW7 2BP, UK.

2. Experimental procedure

2.1. Materials fabrication

A powder blending method was used to fabricate the Al_2O_3-Cr and Al_2O_3-Cr/Ni composites. The starting powders were α-Al_2O_3 AKP-30 powder (Sumitomo Chemical Co. Ltd., Tokyo, Japan), two chromium powders with different particle sizes, 80Cr/20Ni (80 wt% Cr and 20 wt% Ni) powder and 20Cr/80Ni (72 wt% Ni, 16 wt% Cr and 8 wt% Fe) powder. All the metal powders were supplied by Goodfellow Advanced Materials, Cambridge, U.K. Further details are given in Table I. For each blend, the required amounts of alumina and the metallic powder were calculated to give 20 vol% metallic phase in the final composite, assuming full density, no mass loss and no third phase formation. The powder mixture was milled in ethanol using alumina milling media for 24 hours. The slurry was then dried in an oven. The dried powder mixture was crushed and passed through a 200 μm screen. The Al_2O_3-Cr blends were pressureless sintered and, for these experiments, green bodies were formed by uniaxially pressing about 10 g of powder in a 25 mm diameter cylindrical steel die to a pressure of about 30 MPa. Sintering was performed in a tube furnace (Lenton 1850) in air or argon, with or without a surrounding graphite powder bed. The heating rate was 5°C min^{-1}. After holding at the sintering temperature for the required time, the furnace was left to cool naturally to room temperature before the sample was removed. In the hot pressing experiments, about 10 g of the powder blend was hot-pressed in a 25 mm diameter graphite die under argon protection with a ramp rate of 20°C min^{-1}. On reaching 1400°C, a uniaxial pressure of 20 MPa was applied. Both pressure and temperature were held for 30 mins. The pressure was then released and the system cooled to room temperature. The Al_2O_3-Cr powder blend using the coarser chromium powder was not hot-pressed. Sintered and hot pressed samples of monolithic alumina were fabricated for comparison purposes.

2.2. Characterisation of the composites

The densities of the composites were determined by Archimedes' principle. X-ray diffractometry (XRD) using a Philips PW1050 diffractometer with monochromated Cu K_α radiation was used to determine the major phases present in the composites. Microstructural observations of the powder blends, the polished surfaces and fracture surfaces employed scanning electron microscopy (SEM) (Hitachi S3200N) and transmission electron microscopy (TEM). Thin foils for TEM investigations were prepared by standard preparation methods for ceramic materials, i.e., mechanical cutting, dimple grinding/polishing, followed by ion-beam etching. TEM studies were conducted on a Philips CM 200 microscope equipped with an EDX (energy dispersive X-ray) analyser.

TABLE I Particle size and density of the starting powders

Powder	Particle size (μm)	Density (Mg m^{-3})
Al_2O_3	0.3–0.5	3.98
Cr coarse	45–200	7.19
Cr fine	<5	7.19
80Cr/20Ni	<75	7.5
20Cr/80Ni	<75	8.4

2.3. Mechanical property evaluation

Indentation tests were performed using a Vickers pyramid diamond hardness testing machine (Hardness Testing Machines Ltd.). The specimens were polished to a 1 μm diamond surface finish before the tests. A 196 N load with a loading time of 10 seconds was used. Each indentation was placed at least ten diagonal lengths away from adjacent indentations. The average length of radial cracks emanating from the indentation corners was used to obtain a value of fracture toughness using the equation of Liang *et al*. [26]. The fracture toughness results were averaged over 10 indentations per specimen. Double cantilever beam (DCB) testing was used to assess the fracture toughness and resistance-curve behaviour. Typically, the specimens were around 20 mm in length, 12 mm wide and 4 mm thick, with a central grooved area of 1 mm thickness containing a 4 mm long notch. A travelling microscope was used to measure the advancing crack length during the crack opening. Further details of the procedures adopted have been described elsewhere [27].

The flexure strength was evaluated using 3-point bend testing. Bars were cut from the hot pressed bulk and then ground to 2 mm × 1.5 mm × 25 mm. The machining damage was mechanically removed by polishing, ultimately to a 3 μm diamond surface finish on the tensile surface. The other three surfaces were polished to a 30 μm finish. The edges were chamfered to avoid edge defects. The 3-point bend testing was conducted on an Instron 1195 mechanical testing machine using a cross-head speed of 0.5 mm/min and a span of 20 mm. The fracture strength results were averaged over 3–4 specimens.

3. Results and discussion

3.1. Microstructural characterisation of pressureless sintered composites

The sintering or hot pressing schedules and densities of monolithic Al_2O_3 and some of the composites are shown in Table II. Initial work on Al_2O_3-Cr composites made from the coarser chromium powder showed that it was not possible to produce dense samples without the use of a graphite powder bed. An argon atmosphere did not stop the oxidation of the chromium and reaction with the alumina to form an alumina-chromia solid solution. Using a graphite powder bed, it was possible to achieve densities greater than 95% of the calculated theoretical density (TD). The most successful schedule was 1 hour at 1500°C which gave a composite with a density of 4.58 Mg m^{-3} (98.9% TD). XRD of this sample, denoted as SC (sintered, coarse) Al_2O_3-Cr indicated that it contained alumina and chromium as expected but also small amounts of $(Al, Cr)_2O_3$ and chromium carbide. The carbide presumably originated from reaction between the chromium and the graphite powder bed. Microstructural observation of this specimen showed that it was not homogenous. In the outer regions large chromium particles surrounded by many smaller, irregularly-shaped chromium particles could be seen (Fig. 1) whereas the more central chromium

TABLE II Sintering and hot pressing schedules of monolithic Al_2O_3 and the composites

Specimen	Temperature (°C)	Time (mins)	Environment	Density (Mg m^{-3})	Relative density (%)
S Al_2O_3	1500	60	Air	3.88	97.5
SC Al_2O_3-Cr	1500	60	Graphite bed	4.58	98.9
SF Al_2O_3-Cr	1500	60	Graphite bed	4.36	94.2
HP Al_2O_3	1400	30	Graphite die	3.92	98.2
HP Al_2O_3-Cr	1400	30	Graphite die	4.08	98.6
HP Al_2O_3-80Cr/20Ni	1400	30	Graphite die	4.59	99.1[a]
HP Al_2O_3-20Cr/80Cr	1400	60	Graphite die	4.52	99.1[b]

S = sintered, HP = hot pressed.
[a]Based on the measured metal content of 15 vol%.
[b]Based on the measured metal content of 13 vol%.

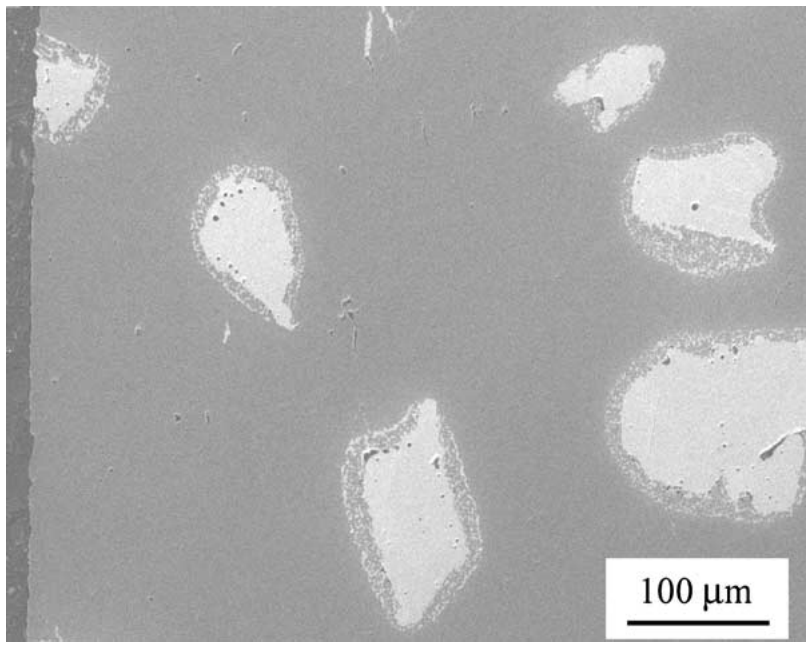

Figure 1 Scanning electron micrograph of large chromium particles surrounded by satellite particles in the outer parts of specimen SC Al_2O_3-Cr.

particles were more regular and did not have satellite particles. EDX of the outer regions indicated that the alumina matrix contained chromium and that there was a higher concentration of carbon associated with the chromium particles. It was possible to produce a TEM foil from this sample (unlike other pressureless sintered materials). Selected area electron diffraction patterns (SADPs) confirmed that the metallic particles were chromium and EDX showed that the chromium content of the matrix decreased with increasing distance from the chromium particles.

It is proposed that the oxygen partial pressure at the start of sintering is sufficiently high for some oxidation of the chromium to take place but that the alumina-chromia solid solution is then reduced to give the satellite chromium particles. Previous work on alumina-nickel composites [4] has shown this type of microstructure to be beneficial in terms of toughness. In order to promote a greater proportion of irregularly shaped chromium particles, a finer chromium powder was used to fabricate composites.

The same sintering schedule as SC Al_2O_3-Cr was used to produce SF (sintered, fine) Al_2O_3-Cr, i.e., 1 hour at 1500°C in a graphite powder bed. This sample was not as dense (4.38 Mg m^{-3}; 94.2%TD) as SC Al_2O_3-Cr and did not exhibit an inhomogeneous microstructure (see Fig. 2).

3.2. Microstructural characterisation of hot pressed composites

It was possible to produce samples with nearly theoretical density by hot pressing. XRD showed that α-Al_2O_3 and Cr were the predominant phases in the Al_2O_3-Cr composite. A peak from chromium carbide may result from interaction between the powder blend and the graphite die used during hot pressing. Fig. 3 is a SEM photomicrograph of this specimen. The Cr particles have a bimodal size distribution. Large Cr particles, about 30 μm in size, and small sub-micrometre Cr particles coexist. Some Cr particles are slightly elongated in the direction perpendicular to the pressing direction. The grain size of the alumina in this sample is about 1.9 μm, which is slightly smaller than that of the monolithic alumina (2.6 μm) fabricated under identical conditions. The alumina powder, however, is in size range 300–500 nm. Thus, alumina grains grew during hot pressing and adding micro-sized Cr inclusions did not inhibit alumina grain growth significantly. The Al_2O_3-Cr/Ni composites show similar microstructural features to the Al_2O_3-Cr composite, in that the metal particles are slightly elongated in the direction perpendicular to the pressing direction. For these composites, the theoretical densities had to be recalculated to take into account the loss of metal during the hot pressing process. With the exception of a slightly higher degree of metal

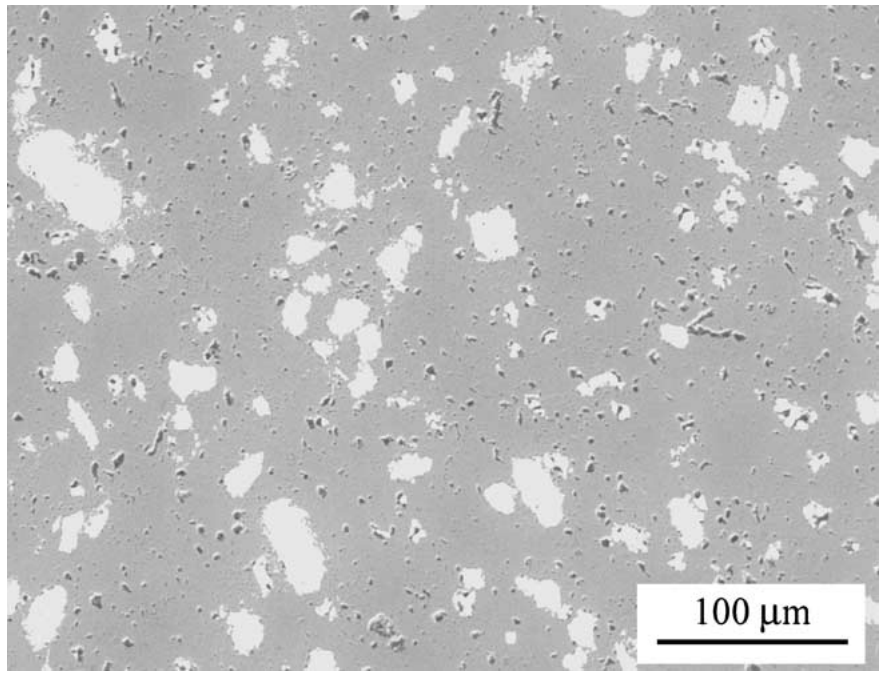

Figure 2 Scanning electron micrograph of the Al_2O_3-Cr specimen made from the fine chromium powder (SF Al_2O_3-Cr), showing a homogeneous microstructure.

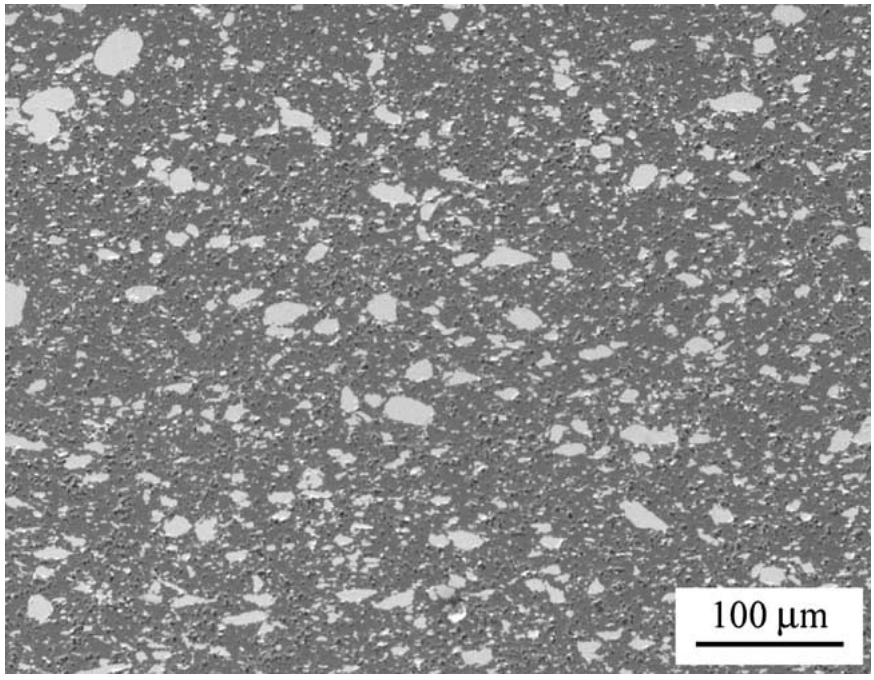

Figure 3 Scanning electron micrograph of the microstructure of the hot pressed Al_2O_3-Cr specimen.

loss in the outer regions, the samples are homogeneous and no interfacial reactions could be detected, although the alumina-metal interfaces were relatively weak and cracked in some instances.

3.3. Mechanical properties

The results of the indentation and strength tests are summarised in Table III. As would be expected, adding a softer metal to alumina produces a composite of lower hardness. The difference between the sintered and hot pressed alumina specimens is probably a result of the finer grain size in the later. The results for the composites are in good agreement, in relative terms, with

TABLE III Mechanical properties of monolithic Al_2O_3 and the composites

Specimen	Hardness (GPa)	Indentation fracture toughness (MPa $m^{1/2}$)	Strength (MPa)
S Al_2O_3	16.3 ± 0.4	3.2 ± 0.2	320 ± 25
SC Al_2O_3-Cr	13.0 ± 1.1	5.0 ± 0.7	181 ± 8
SF Al_2O_3-Cr	12.7 ± 0.6	6.2 ± 0.8	264 ± 27
HP Al_2O_3	17.5 ± 0.8	3.4 ± 0.2	476 ± 17
HP Al_2O_3-Cr	12.0 ± 0.8	7.1 ± 1.1	440 ± 30
HP Al_2O_3-80Cr/20Ni	12.7 ± 0.4	6.6 ± 0.7	353 ± 38
HP Al_2O_3-20Cr/80Cr	11.9 ± 0.2	6.8 ± 0.6	418 ± 11

the values reported by Guichard *et al*. [14] for 22 vol% Cr composites, although their actual values are higher. Indentation testing was also used to investigate the potential benefits of adding metal particles in terms of the fracture toughness behaviour. Indentation fracture toughness values can be somewhat different from those obtained from more conventional tests and in this case it was difficult to obtain well-formed indentations in the composites so the values can be used only as indications of behaviour. The two alumina materials have essentially the same fracture toughness value and all of the composites have higher values, indicating that some toughening mechanism is in operation. Again, the values are comparable with those reported by others. Guichard *et al*. [14], using a single edge notched beam technique, report values of 3 and 4.3 MPa $m^{1/2}$ for alumina and Al_2O_3-22 vol% Cr, respectively whilst Laurent *et al*. [13] report a value of 4.5 MPa $m^{1/2}$ for alumina and 7.5 MPa $m^{1/2}$ for Al_2O_3-20 vol% Cr, as measured using an indentation strength technique.

In metallic particle toughened systems, the most benefit, in terms of toughness behaviour, is derived from plastic deformation of metallic ligaments bridging the opening crack. Examination of the indentation cracks did not reveal more than one or two particles spanning the crack. Rather, the preferred crack paths were either along the metal/alumina interface, indicating that this is an area of weakness, or through the metal particles in the case of Cr and 80Cr/20Ni (see Fig. 4). Thus, the toughening increment is most likely to derive from

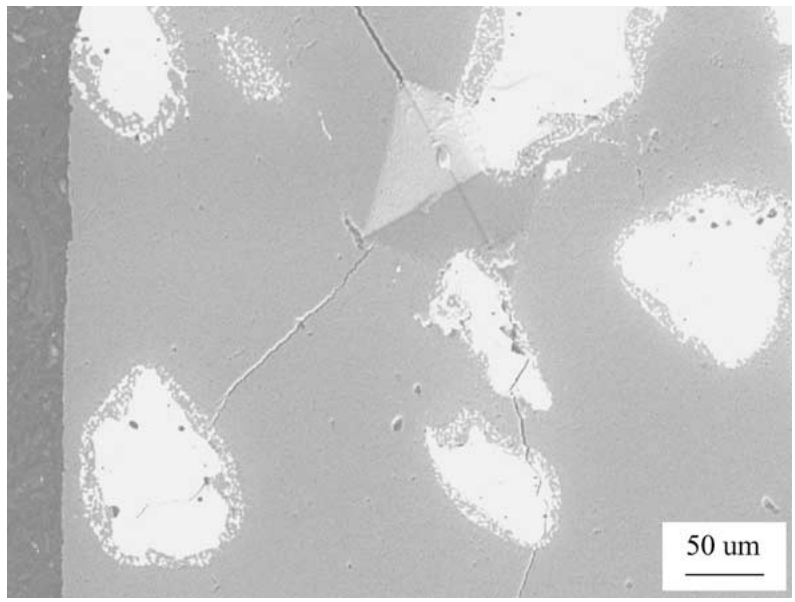

(a)

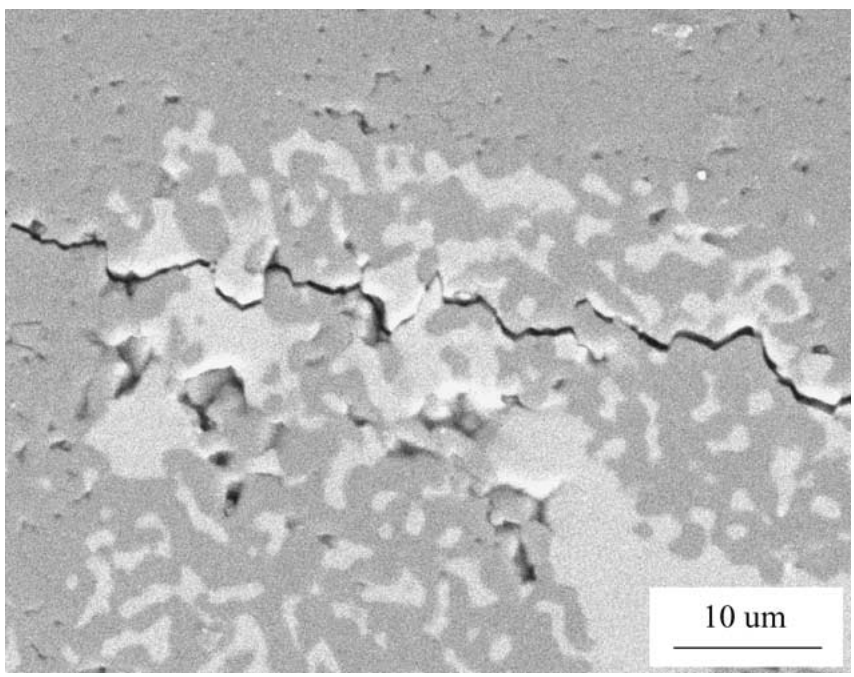

(b)

Figure 4 Scanning electron micrographs showing (a) the interaction of indentation cracks with Cr particles and (b) a higher magnification view of the region of small Cr particles surrounding a larger Cr particle in SC Al_2O_3-Cr. Note that the cracks either travel along the metal-alumina interface or through the metallic particles.

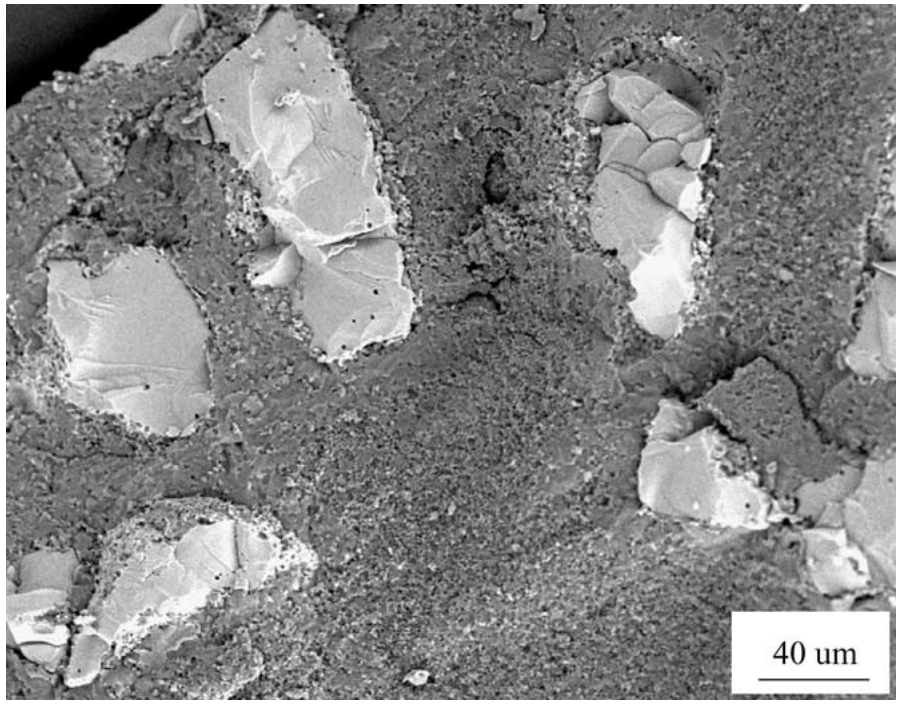

(a)

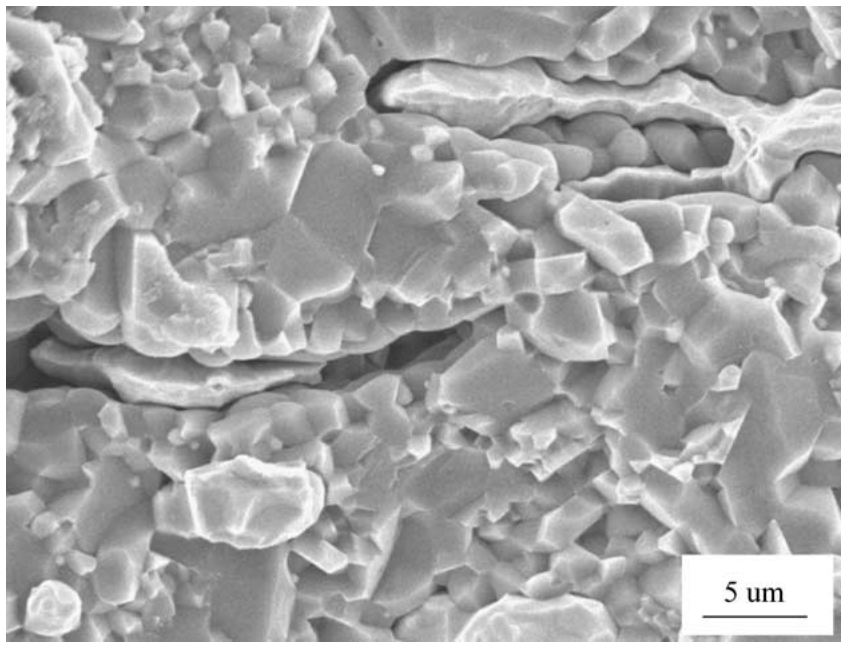

(b)

Figure 5 Fracture surfaces of (a) SC Al_2O_3-Cr and (b) HP Al_2O_3-20Cr/80Cr. Note that the Cr particles have fractured in a brittle manner whereas the 20Cr/80Ni particles show evidence of necking prior to failure.

crack deflection and the maximum potential benefit is not being gained from metal particle inclusion.

The flexure strength values for the materials are also given in Table III. All of the hot-pressed materials have higher strengths than the sintered materials. The hot pressed alumina is stronger than the sintered alumina, presumably on account of its finer grain size. The sintered composites are weaker than the sintered alumina, with SC Al_2O_3-Cr exhibiting the lowest strength of all of the materials. The weak interfacial bonding is likely to mean that the strength-limiting defects are comparable with the size of the chromium particles. The hot pressed composites are also weaker than the hot pressed alumina, probably for the same reasons as above. Examination of the fracture surfaces showed that cleavage through the metal particles had occurred in the cases of Cr and 80Cr/20Ni but not 20Cr/80Ni (see Fig. 5). The fracture strengths measured here are lower than those reported by Guichard *et al*. [14] and Laurent *et al*. [13], who both report that the composites are stronger than the parent alumina by factors of 1.6 and 2.2, respectively. Further, Guichard *et al*. note that the interfacial bonding is strong, contrary to the observations in this work, and in both cases a significant fraction of the metallic particles are in the submicrometre size range.

Weak metal/ceramic bonding is a well-known problem in these systems but fracture through the metal is not often reported. Chromium and 80Cr/20Ni have the

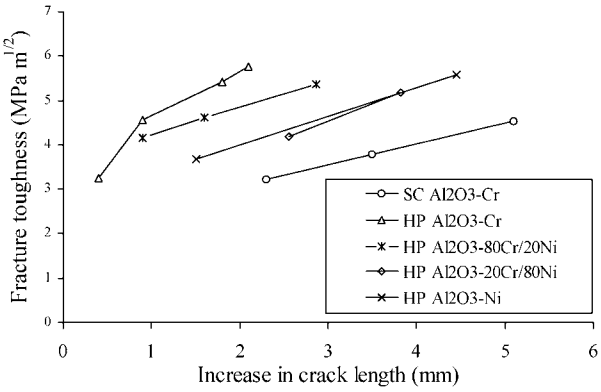

Figure 6 Results of the double cantilever beam testing showing that all of the composites exhibit resistance-curve behaviour in that fracture toughness increases with increasing crack length.

body-centred cubic crystal structure and as such show a brittle to ductile transition, which is temperature dependent. For chromium, this temperature is above room temperature and shows a very sharp transition from brittleness to ductility over a range of only a few degrees of temperature [28]. It has been found that chromium has a greater tendency to fail by cleavage than other body-centred cubic metals [29]. The propensity for brittleness is enhanced by the presence of impurities, such as nitrogen, oxygen and carbon [30–32]. In particular, carbon contents as low as 0.01% have been reported to lead to brittle fracture at room temperature. An impurity level of 0.02% carbon is reported, by the manufacturer, to be associated with the starting powders and further carbon could be introduced from the graphite powder bed or die used in the densification procedures. Further, in the SEM EDX investigation of SC Al_2O_3-Cr, carbon was found to be associated with the chromium particles. Thus, it is reasonable to conclude that the presence of carbon has resulted in the embrittlement of the predominantly chromium metallic particles. When more nickel is present, as in the case of 20Cr/80Ni, a face-centred cubic structure is adopted, and the particles should show ductile failure at all temperatures.

In order to examine the fracture toughness behaviour more rigorously, DCB testing was attempted although the inherent experimental difficulties associated with this technique meant that only one sample per material was tested. The results are given in Fig. 6, along with data on an Al_2O_3-Ni composite from previous work [4]. The DCB values are lower than the indentation fracture toughness values at comparable crack lengths. All of the composites show resistance-curve behaviour in that the fracture toughness is a function of crack length. None of the curves have reached a plateau, indicating that the process zones are not developed fully, even when the cracks are a few millimetres in length. Previous work on the parent alumina [12] has shown it to possess a flat resistance-curve with a constant fracture toughness of around 3 MPa m$^{1/2}$. In terms of this limited data, the HP Al_2O_3-Cr is the best material, in that the fracture toughness increases most rapidly with crack length and reaches the highest value. This is contrary to the predictions of behaviour arising from the indentation crack path and fracture surface studies. On the basis of these results, HP Al_2O_3-20Cr/80Ni would have been expected to exhibit ductile particle stretching during the DCB testing, which should have produced a greater toughening increment than crack deflection in the other composites. This behaviour may be a consequence of the difference in the particle sizes in the two materials. The finer scale microstructure in the HP Al_2O_3-20Cr material may lead to a shorter process zone. Hence, it is possible that had longer crack lengths been investigated then the maximum fracture toughness value of HP Al_2O_3-20Cr/80Ni could have been the highest of all the materials. Further work is needed to clarify these issues.

The results of indentation testing and DCB testing are in broad agreement in that both methods indicate that the composites are tougher than the parent alumina. It would appear that the residual stresses around the particles, resulting from the mismatch in the coefficients of thermal expansion, have little effect on the fracture toughness behaviour, in that all of the composites show similar behaviour even though the coefficients of thermal expansion of the metallic phases are quite different. Thus, other factors are controlling the behaviour. Carbon embrittlement of chromium and 80Cr/20Ni leads to cleavage fracture of some particles. This is most pronounced in the SC Al_2O_3-Cr composite, presumably as a result of the graphite powder bed. In all composites, the weak metal-alumina interface, however, is the major factor preventing the full utilisation of the metallic phase.

4. Conclusions

The microstructures and the mechanical properties of a range of Al_2O_3-Cr and Al_2O_3-Cr/Ni composites have been examined. Dense composites can be manufactured by pressureless sintering in the presence of a graphite bed or by hot pressing. All of the composites were found to be tougher than the parent alumina and to show resistance-curve behaviour. Fracture surface examination showed the full toughening potential of the metal particles was not exploited to any significant extent, principally due to the weak metal-Al_2O_3 interface, but also because of carbon embrittlement of the chromium and 80Cr/20Ni phases. Further, this weak interfacial bonding is also likely to be responsible for the relatively low strength values of the composites.

Acknowledgements

Ying Ji is grateful to the former School of Mechanical and Materials Engineering, University of Surrey for the financial support to undertake this work.

References

1. E. BREVAL, Z. DENG, S. CHIOU and C. G. PANTANO, *J. Mater. Sci.* **27** (1992) 1464.
2. E. BREVAL and C. G. PANTANO, *ibid.* **27** (1992) 5463.
3. W. H. TUAN and R. J. BROOK, *Journal of the European Ceramic Society* **6** (1990) 31.
4. X. SUN and J. YEOMANS, *J. Amer. Ceram. Soc.* **79** (1996) 2705.
5. T. SEKINO, T. NAKAJIMA, S. UEDA and K. NIIHARA, *ibid.* **80** (1997) 1139.
6. R. Z. CHEN and W. H. TUAN, *Journal of the European Ceramic Society* **19** (1999) 463.

7. J. LU, L. GAO, J. SUN, L. GUI and J. GUO, *Materials Science and Engineering*, A **293** (2000) 223.
8. M. LIEBERTHAL and W. D. KAPLAN, *ibid.* A **302** (2001) 83.
9. S.-T. OH, M. SANDO and K. NIIHARA, *J. Amer. Ceram. Soc.* **81** (1998) 3013.
10. *Idem.*, *Scripta Mater.* **39** (1998) 1413.
11. J. L. GUICHARD, O. TILLEMENT and A. MOCELLIN, *J. Mater. Sci.* **32** (1997) 4513.
12. P. A. TRUSTY and J. A. YEOMANS, *Journal of the European Ceramic Society* **18** (1998) 495.
13. CH. LAURENT, A. PEIGNEY, O. QUÉNARD and A. ROUSSET, *Sil. Ind.* **63** (1998) 77.
14. J. L. GUICHARD, O. TILLEMENT and A. MOCELLIN, *Journal of the European Ceramic Society* **18** (1998) 1743.
15. W. B CHOU and W. H. TUAN, *Journal of the European Ceramic Society* **15** (1995) 291.
16. O. SBAIZERO and G. PEZZOTTI, *Journal of the European Ceramic Society* **20** (2000) 1145.
17. M. NAWA, T. SEKINO and K. NIIHARA, *J. Mater. Sci.* **29** (1994) 3185.
18. J. LU, L. GAO, J. GUO and K. NIIHARA, *Materials Research Bulletin* **35** (2000) 2387.
19. D. E. ALDRICH and M. J. EDIRISINGHE, *J. Mater. Sci. Lett.* **17** (1998) 965.
20. S-T. OH, T. SEKINO and K. NIIHARA, *Journal of the European Ceramic Society* **18** (1998) 31.
21. S-T. OH, J-S. LEE, T. SEKINO and K. NIIHARA, *Scripta Mater.* **44** (2001) 2117.
22. T. SEKINO and K. NIIHARA, *Nanostructured Materials* **6** (1995) 663.
23. *Idem.*, *J. Mater. Sci.* **32** (1997) 3943.
24. Y. S. TOULOUKIAN, R. K. KIRBY, R. E. TAYLOR and P. D. DESAI (Eds.) in "Thermophysical Properties of Matter," The TPRC Data Series, Vol. 12: Thermal Expansion—Metallic Elements and Alloys (Plenum, New York, 1975) p. 61.
25. Y. S. TOULOUKIAN, R. K. KIRBY, R. E. TAYLOR and T. Y. R. LEE (Eds.) in "Thermophysical Properties of Matter," The TPRC Data Series, Vol. 13: Thermal Expansion—Non-Metallic Solids (Plenum, New York, 1977) p. 176.
26. K. M. LIANG, G. ORANGE and G. FANTOZZI, *J. Mater. Sci.* **25** (1990) 207.
27. P. A. TRUSTY, Ph. D. thesis, University of Surrey, UK, 1994.
28. A. H. SULLY, E. A. BRANDES and K. W. MITCHELL, *Journal of the Institute of Metals* **81** (1952/1953) 585.
29. C. GANDHI and M. F. ASHBY, *Acta Metallurgica* **27** (1979) 1565.
30. B. C. ALLEN, D. J. MAYKUTH and R. I. JAFFEE, *Transaction of the Metallurgical Society of AIME* **227** (1963) 724.
31. R. E. CAIRNS JR. and N. J. GRANT, *ibid.* **230** (1964) 1150.
32. H. L. WAIN and S. T. M. JOHNSTONE, *Journal of the Institute of Metals* **83** (1954/1955) 133.

Received 4 December 2001
and accepted 18 July 2002